

Branching Ratios for the Decay of Vector Mesons into Lepton Pairs*

S. S. HERTZBACH,[†] R. W. KRAEMER,[‡] L. MADANSKY, AND R. A. ZDANIS
The Johns Hopkins University, Baltimore, Maryland

AND

R. STRAND

Brookhaven National Laboratory, Upton, New York

(Received 19 July 1966)

We have studied the decays into lepton pairs of vector mesons (ρ , ϕ , ω) produced by a beam of 3-BeV/ c π^- mesons incident on a liquid- H_2 target at the Brookhaven AGS. The experiment utilized scintillation counters and spark chambers as well as a lead-scintillator "shower chamber" constructed for the identification of electrons and rejection of background. A Monte Carlo technique was used to predict the background and determine the number of real events. For the muon-pair mode, the results are upper limits, with the branching ratio ($\rho \rightarrow \mu\bar{\mu}$)/($\rho \rightarrow$ all modes) $< 14 \times 10^{-4}$ being the best limit determined. For the electron-pair decays we obtain ($\rho \rightarrow e\bar{e}$)/($\rho \rightarrow$ all modes) $= (0.65_{-0.5}^{+1.1}) \times 10^{-4}$ and ($\omega \rightarrow e\bar{e}$)/($\omega \rightarrow$ all modes) $= (1.0_{-0.75}^{+1.7}) \times 10^{-4}$ for an assumed ϕ - ω mixing angle of 38° . Because of insufficient knowledge of the production process, we tentatively quote for the ϕ meson a result $\sigma_\phi \times (\phi \rightarrow e\bar{e})/(\phi \rightarrow$ all modes) $= 0.31_{-0.21}^{+0.34} \mu\text{b}$. The results are compared with other experiments.

I. INTRODUCTION

WE report here further details of an experimental study of the decays of the neutral vector mesons (ρ , ϕ , ω) into lepton pairs.¹ Shortly after the observation of the ρ and ω mesons as spin 1⁻ multipion resonances the importance of studying their electromagnetic decays, in particular the lepton-pair mode, was noted by several authors.^{2,3} The observation of the ϕ meson and early speculations concerning ω - ϕ mixing⁴ created additional interest in such experiments. In addition to the predictions made concerning the decay rates,²⁻⁶ these decay processes are of theoretical interest because of their relation to the electromagnetic form factors of the nucleon^{2,5} and the possibility of detecting a difference between the electron and muon interactions.³

Previous experiments,⁷ utilizing both hydrogen and heavy-liquid bubble chambers, provided an estimate

* Work supported by the National Science Foundation, U. S. Atomic Energy Commission, and U. S. Air Force Office of Scientific Research.

[†] Present address: Department of Physics, University of Massachusetts, Amherst, Massachusetts. This material represents part of a dissertation submitted in partial fulfillment of the requirements for the degree of Doctor of Philosophy to the Physics Department of The Johns Hopkins University.

[‡] Present address: Department of Physics, Carnegie Institute of Technology, Pittsburgh, Pennsylvania.

¹ R. A. Zdanis, L. Madansky, R. W. Kraemer, S. Hertzbach, and R. Strand, *Phys. Rev. Letters* **14**, 721 (1965).

² Y. Nambu and J. J. Sakurai, *Phys. Rev. Letters* **8**, 79 (1962); M. Gell-Mann, D. Sharp, and W. G. Wagner, *ibid.* **8**, 261 (1962).

³ G. Feldman, T. Fulton, and K. C. Wali, *Nuovo Cimento* **24**, 278 (1962); E. D. Zhizhin and V. V. Solov'ev, *Zh. Eksperim. i Teor. Fiz.* **43**, 268 (1962) [English transl.: *Soviet Phys.—JETP* **16**, 192 (1963)]; J. Baroff and T. Fulton, *Nuovo Cimento* **29**, 687 (1963).

⁴ J. J. Sakurai, *Phys. Rev. Letters* **9**, 472 (1962); J. J. Sakurai, *Phys. Rev.* **132**, 434 (1963); S. L. Glashow, *Phys. Rev. Letters* **11**, 48 (1963); S. Okubo, *Phys. Letters* **5**, 165 (1963).

⁵ R. F. Dashen and D. H. Sharp, *Phys. Rev.* **133**, B1585 (1964).

⁶ J. B. Bronzan and F. E. Low, *Phys. Rev. Letters* **12**, 522 (1964).

⁷ J. J. Murray *et al.*, *Phys. Letters* **7**, 358 (1963); V. V. Barmin, A. G. Dolgolenko, Yu. S. Krestnikov, A. G. Meshkovskii, and

of the upper limit for the branching ratios to some of the lepton-pair decay modes. The current experiment, designed to be sensitive to branching ratios as small as 10^{-4} , was performed at the Brookhaven AGS using scintillation counters and spark chambers. Vector mesons (V^0) were produced via the reaction $\pi^- + p \rightarrow n + V^0$ with a beam of negative pions incident on a liquid-hydrogen target, and the lepton pairs from subsequent decays were detected by the counter system. The electrons were identified and distinguished from pions by "shower chambers" designed for this purpose and constructed of lead and plastic scintillator.

II. EXPERIMENTAL PROCEDURE

In Fig. 1 the experimental apparatus for identification of lepton pairs is shown schematically. The liquid-hydrogen target was 4 in. in diameter and 18 in. long, and the vacuum tank had a Mylar exit window large enough to accept particles leaving the target at an angle of 30° with respect to the beam direction. A, B, and B* each represents an array of four scintillation counters arranged about the beam axis as shown in the

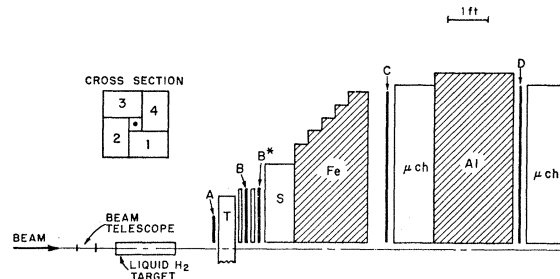


FIG. 1. Experimental apparatus. (One-half of the apparatus is shown.)

V. A. Shebanov, *Zh. Eksperim. i Teor. Fiz.* **45**, 2082 (1963) [English transl.: *Soviet Phys.—JETP* **18**, 1427 (1964)]; A. Bezaquet *et al.*, *Phys. Letters* **12**, 70 (1964); A. Barbaro-Galtieri and R. D. Tripp, *Phys. Rev. Letters* **14**, 279 (1965).

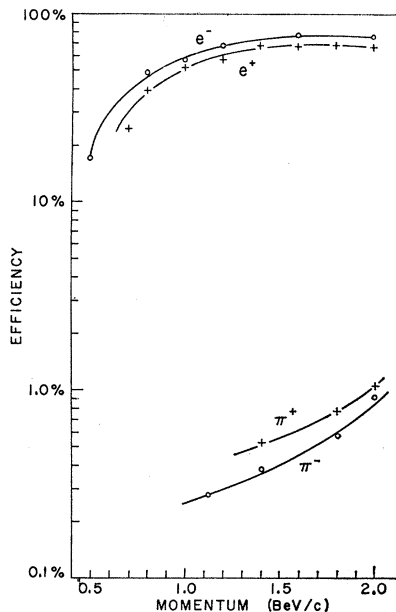


FIG. 2. Singles counting efficiencies for the electron detectors (counters B and B* and the shower chamber).

cross section, and S represents a similar array of "shower chambers" used to identify electrons. A 4×4-in. beam hole was maintained throughout the apparatus in order to minimize singles counting rates and accidental coincidences. The 24×24×4.5-in. thin-plate spark chamber (T) was placed near the front of the system so that the tracks of the pair could be observed before appreciable material was encountered. In view of the small branching ratios involved, the apparatus was designed to have a large solid angle of acceptance. The solid angle was equal to that subtended by a range of 24° in the polar angle and 360° in azimuth.

Counters B and B* and the shower chambers provided electronic identification of electrons and rejection of pion background by virtue of the shower phenomenon. The pion-pair background from the 2π decay of the ρ meson alone is expected to be a few millibarns while the lepton-pair signal is expected to be several orders of magnitude smaller. The singles efficiency curves obtained when signals from B, B*, and the shower chamber were subjected to pulse-height discrimination are shown in Fig. 2, indicating an electron-pair efficiency which is about 10^4 times that for pion pairs. (Details of the construction and calibration of the shower chambers are presented in the Appendix.) In addition to using the anode signals for pulse-height discrimination, the ten dynode signals from each shower chamber were added to provide a "sum pulse" which served as a measure of the energy of the incident electron.

A coincidence between two A counters, two B counters, and the beam telescope identified a pair emerging from the target. An additional coincidence was required to form a trigger for an "electron-pair"

event, indicating that the pulse-height criteria set up to identify electrons were satisfied in two quadrants. For each such trigger, the sum pulses from all four shower chambers were displayed on an oscilloscope and the traces photographed in addition to the spark chambers and μ/e trigger indicators.

The apparatus behind the shower chambers was for the identification of muon pairs. Following the 22 in. of iron (2.75 pion mean free paths) was an array C of 8 counters approximating a circle 6 ft in diameter. The aluminum spark chambers (muon chambers designated in Fig. 1 as μ ch) and absorber amounted to another 1.25 mean free paths of material preceding the D counters, a 16-counter array measuring 8×8 ft. Since many of the muons produced would have had momenta low enough to be stopped by this much material, the initial logic called for signals from two C counters and one D counter, in coincidence with the signal identifying a pair emerging from the target, to form a trigger for a "muon-pair" event. The Monte Carlo calculations indicated that this arrangement would result in an average rejection of pion pairs over muon pairs by a factor of 10^4 . Experimental difficulties (primarily the difficulty of timing the large array of 16 D counters with very low counting rates) prevented the incorporation of the D counters into the electronic logic. Subsequent Monte Carlo calculations indicated that this resulted in an increase of the electronic acceptance of pion-pair contamination by a factor of 20.

The pion beam was taken from the G-10 target (a 0.030×0.030×6-in. beryllium wire) at an angle of 10.5° with respect to the AGS internal proton beam and focused at the momentum defining slit by a quadrupole doublet. The $\frac{3}{4}$ ×4-in. collimating slit 34 ft downstream from a bending magnet limited the beam momentum to 3.0 BeV/c±1%. A second quadrupole doublet and another bending magnet further defined the beam and rendered it parallel to the beam line as it passed through the 4×4-in. opening in the spark chamber-counter array. Using a ratio of $\pi^-/K^- = 10$ at the G-10 target⁸ and a total flight path of 185 ft, the kaon contamination at the hydrogen target was calculated to be ≈1%. The muon contamination was found to be ≈10% by attenuation measurements on the beam. The beam flux, in the momentum band and spatial region indicated, was about 2.5×10^5 pions/sec per 10^{11} protons during a 150-msec gate interval.

III. ANALYSIS OF DATA—MONTE CARLO CALCULATIONS

The data-reduction process required that the photographs of the oscilloscope display show exactly two sum pulses in the proper position for coincidence. For electron triggers these pulses were required to be larger than the cutoff determined by the shower-chamber calibration, and for muon triggers they were required to

⁸ W. F. Baker *et al.*, Phys. Rev. Letters 7, 101 (1961).

correspond to minimum ionizing particles. The photographs of the tracking chamber (T) were required to show two tracks consistent with the quadrants for which the shower chamber showed pulses. The tracking-chamber photographs for events meeting these criteria were measured on a film-plane measuring machine. The reconstructed tracks were required to have a common origin within the liquid-hydrogen target and were again checked for consistency with the oscilloscope traces.

The result of the data-reduction process is a histogram showing the distribution of opening angles for those events which were accepted as bona fide examples of pairs, and includes both lepton pairs and a small fraction of the pion pairs produced. The opening-angle distribution expected to result from a particular physical process is a function of the momentum and mass of the decaying particle as well as the decay angular distribution and the mass of the decay products. The Monte Carlo technique was employed as a means of integrating the expected opening-angle distribution over the momentum spectrum and decay angular distribution of the decaying particle. The acceptance of the detection apparatus was folded into the calculation. The integration over momenta incorporated the production angular distribution and, in the case of a broad resonance, the mass spectrum of the resonance under consideration. In the case of pairs produced according to phase space, the proper mass distribution was incorporated. The distributions for production and decay were obtained from the references in Table I. The resulting opening-angle distributions are still correlated with the masses of the decaying system and the decay products. The same calculation determined the efficiency of the system for detecting pairs produced by the process under consideration. The decay into lepton pairs was assumed to be isotropic in the rest frame of the decaying particle.

TABLE I. Processes considered in generating Monte Carlo events.

Process ^a	Cross section ^b (mb)	Reference
$\pi^- + p \rightarrow \pi^- + p$	6.8	c
$n + \eta$	0.05	d
$n + \rho^0$	1.6	e, f
$n + \omega$	0.5	d, g, h
$n + \phi$?	
$n + f^0$	0.32	e, f
$N^* + \pi + \pi$	0.8	f
$N + \pi + \pi$	1.3	f
$N + \pi + \pi + \pi$	0.9	f
$p + \rho^-$	0.7	f
$\Sigma^0 + K^0$	0.086	i
$\Lambda^0 + K^0$	0.031	i
$\Sigma^- + K^+$	0.015	i
$n + \pi^0$	0.3 ^j	k

- ^a N represents either neutron or proton.
^b Branching ratios to various modes are from A. Rosenfeld *et al.*, Rev. Mod. Phys. **36**, 977 (1964), except where explicitly stated.
^c W. Selove (private communication).
^d W. Bugg (private communication). Branching ratio to Dalitz pairs from T. Fulton (private communication); and D. Bessis, W. Jacob, and A. Morel, Nuovo Cimento **30**, 112 (1963).
^e W. Selove, V. Hagopian, H. Brody, A. Baker, and E. Leboy, Phys. Rev. Letters **9**, 272 (1962).
^f V. Hagopian (private communication).
^g R. Kraemer *et al.*, Phys. Rev. **136**, B496 (1964).
^h U. Kruse (private communication).
ⁱ T. Wangler, A. Erwin, and W. Walker, Phys. Rev. **137**, B414 (1965).
^j mb/sr at 0°.
^k M. Whalig *et al.*, Phys. Rev. Letters **13**, 103 (1964).

The resulting distribution for each process was averaged over the target volume and folded into a resolution function. The curves for all processes were added together, each being weighted in proportion to the product of production cross section (σ_{prod}), branching ratio (B), and detection efficiency (E). This was done both with and without the inclusion of direct lepton-pair decays. Comparison of these curves, as described below, allows a determination of the rates for direct lepton-pair decays to be made.

The processes considered as sources of background are listed in Table I. We once again list, in Table II,

TABLE II. Monte Carlo results.

	Electron pairs			Muon pairs	
	E	σ_{eff} ($10^{-3}\mu\text{b}$)	θ_{peak} (deg)	E	σ_{eff} ($10^{-3}\mu\text{b}$)
(a) Background processes					
$\pi^- p \rightarrow n\rho^0 (\rightarrow \pi^+\pi^-)$	3.25×10^{-6}	4.9	28.0	1.42×10^{-4}	213
$n\rho^0 (\rightarrow \pi\mu\bar{\nu})$	28.5	0.75×10^{-4}	113
$n\pi^+\pi^-$	0.86×10^{-6}	1.1	26.5	0.59×10^{-4}	77
$N^*\pi^+\pi^-$	1.07×10^{-6}	0.9	19.0	0.65×10^{-4}	52
$n\pi^0 (\rightarrow \gamma\gamma)$	5.42×10^{-6}	2.7	6.5
$n\eta (\rightarrow \gamma\gamma)$	32.1×10^{-6}	1.0	22.0
$n\eta (\rightarrow \gamma e\bar{e})$	1.2×10^{-2}	6.0	21.0
$(\Lambda^0/\Sigma^0)K^0 (\rightarrow \pi^+\pi^-)$	2.3×10^{-6}	0.1	19.0
Total σ_{eff}		16.7			455
(b) Lepton pair decays					
$\pi^- p \rightarrow n\rho^0 (\rightarrow e\bar{e})$	0.098	...	30.0
$n\rho^0 (\rightarrow \mu\bar{\mu})$	29.0	0.15	...
$n\omega (\rightarrow e\bar{e})$	0.048	...	30.5
$n\omega (\rightarrow \mu\bar{\mu})$	30.0	0.075	...
$n\phi (\rightarrow e\bar{e})$	0.026	...	40.5
$n\phi (\rightarrow \mu\bar{\mu})$	39.8	0.040	...

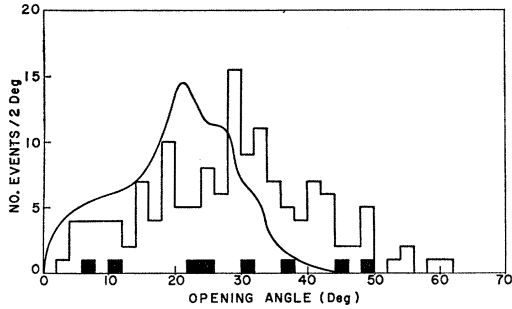


FIG. 3. Histogram of electron data as a function of pair opening angle. The shaded events are the target-empty data, and the solid curve is the distribution generated via the Monte Carlo technique for background processes.

those processes which the Monte Carlo calculation showed to be the major sources of events. For each of these cases we also list the detection efficiency as calculated by the Monte Carlo program, the effective cross section (defined as $\sigma_{\text{eff}} = \sigma_{\text{prod}} \times B \times E$), and the peak or central value of the corresponding distribution.

The histogram in Fig. 3 shows the distribution of pair opening angles for 143 electron-pair events corresponding to 1.2×10^9 pions incident upon the hydrogen target. The photographs obtained with 0.56×10^9 pions incident on the empty target were treated in exactly the same manner, yielding the eight events shown shaded in Fig. 3. The solid curve in Fig. 3 shows the distribution expected to result from background processes as calculated by the Monte Carlo program.

In order to check the angular calibration of the Monte Carlo program, we used the geometric selection of the detection system to generate an opening-angle distribution of track pairs. A distribution calculated with the Monte Carlo program to simulate accidental coincidences of pions from π^-p elastic scattering was compared with one obtained from the experimental data by pairing tracks from different events, resulting in uncorrelated pairs. These curves are shown in Fig. 4 and support the general validity of the Monte Carlo technique used.

The opening-angle distributions generated by the Monte Carlo calculation for electron-pair decays of the ρ and ω mesons were similar enough that they could not be distinguished from each other in the current experiment; hence, we cannot separate $\rho \rightarrow e\bar{e}$ events from $\omega \rightarrow e\bar{e}$ events. However, we will take this opening-angle distribution, appropriate for both ρ and ω decays, add it to that shown in Fig. 3 for background, and again compare with the experimental distribution.

If the curve is normalized to the same number of events as in the experimental distribution, there is a single parameter, namely the ratio of ρ and ω to background events, which may be chosen to give a least-squares fit. The resulting curve is shown in Fig. 5. The dashed curve indicates the background contribution which is 53% of the total. We note that the worst part

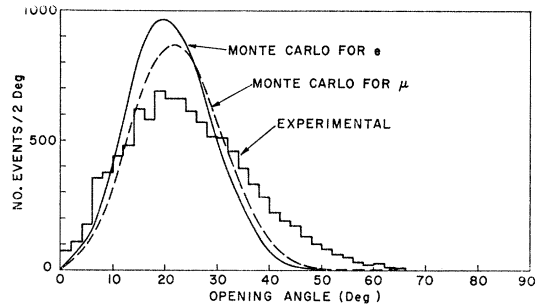


FIG. 4. Distribution of opening angles for Monte Carlo calibration.

of the fit is in the region of angles greater than 40° . Electron-pair decays of the ϕ meson result in a distribution peaked about 40° . We tentatively identify the majority of the events above 35° with this decay mode of the ϕ meson.

The inclusion of the ϕ decay mode contributes an additional fitting parameter, the ratio of ϕ decays relative to the background. We conclude that the corresponding distribution, shown as the solid curve in Fig. 6 is the best over-all fit to the data. The parameters extracted from this fit are used to determine the branching ratios.

The results of the curve fitting are summarized in Table III. The nature of the fits obtained is independent of the size and manner of choice of the histogram bins.

IV. RESULTS

The Monte Carlo calculation yields an effective cross section for all background processes of $(16.7 \pm 2.5) \times 10^{-3} \mu\text{b}$, and the fit to the experimental data implies that this corresponds to 50% of all the events. Thus, we can compute a total effective cross section of $(33.4 \pm 5.0) \times 10^{-3} \mu\text{b}$ (where the error does not include any uncertainty in the absolute efficiencies calculated).

The detected number of events of a given type is proportional to the product of production cross section, branching ratio, and detection efficiency. As indicated in Table III, 30% of the events are due to ρ and ω decays into electron pairs. To divide ρ and ω events properly and to determine the branching ratio for $\rho \rightarrow e\bar{e}$, we can write

$$\sigma_\rho B_\rho E_\rho [1 + (\sigma_\omega/\sigma_\rho)(E_\omega/E_\rho)(B_\omega/B_\rho)] = 0.3 \times (33.4 \times 10^{-3}) \mu\text{b}. \quad (1)$$

Both B_ω and B_ρ are unknown, but if we make use of the results of unitary symmetry and ω - ϕ mixing theory,^{2,4,5} we can write

$$B_\omega/B_\rho = \frac{1}{3} (M_\omega/M_\rho) (\Gamma_\rho/\Gamma_\omega) \sin^2\theta, \quad (2)$$

where M_ω/M_ρ is the ratio of the masses of the ω and ρ mesons, $\Gamma_\rho/\Gamma_\omega$ is the ratio of the total widths of the ρ and ω , and θ is the ω - ϕ mixing angle. Then we have,

TABLE III. Normalized fits.

	No. deg. of freedom	χ^2	Prob.	Background	Fraction (ρ and ω)	ϕ
Background only	31	112	10^{-9}	1.0
Background+ (ρ and ω)	30	55	0.005	0.53 ± 0.10	0.47 ± 0.10	...
Background+ (ρ and ω) + ϕ	29	29	0.46	0.50 ± 0.07	0.30 ± 0.07	0.20 ± 0.05

approximately, for the above:

$$\sigma_{\rho} B_{\rho} E_{\rho} [1 + 0.7 \times \sin^2 \theta] = 10^{-2} \mu\text{b}. \quad (1')$$

with

$$B_{\omega}/B_{\rho} = 3.8 \sin^2 \theta. \quad (2')$$

Using the value $\theta = 38^{+2.4, -4.5}$ we compute

$$\begin{aligned} B(\rho \rightarrow e\bar{e}) &= (0.65_{-0.5}^{+1.1}) \times 10^{-4}, \\ B(\omega \rightarrow e\bar{e}) &= (1.0_{-0.75}^{+1.7}) \times 10^{-4}. \end{aligned} \quad (3)$$

The Monte Carlo calculation yields an effective cross section which differs by 30% from the observed cross section determined from accepted events. The above errors are primarily the reflection of this uncertainty in absolute normalization upon the Monte Carlo calculations. The contribution from statistical errors is small. Similarly, we obtain for the ϕ events

$$\sigma_{\phi} \times B(\phi \rightarrow e\bar{e}) = (0.31_{-0.21}^{+0.34}) \mu\text{b}. \quad (4)$$

We leave this result in the form of a product since we do not know the ϕ -production cross section in 3-BeV/c π^-p interactions, although some recent work⁹ indicates that the value may be about $50 \mu\text{b}$ for incident pion momenta of about 2 BeV/c but considerably less for momenta above 2.6 BeV/c. If the cross section is indeed this small, then the branching ratio $B(\phi \rightarrow e\bar{e})$ appears larger than the SU_3 prediction. However, we would withhold a definite statement pending better knowledge of the production process, since the interpretation of the data depends strongly on the production cross section and the angular distribution used in the Monte Carlo calculation.¹⁰

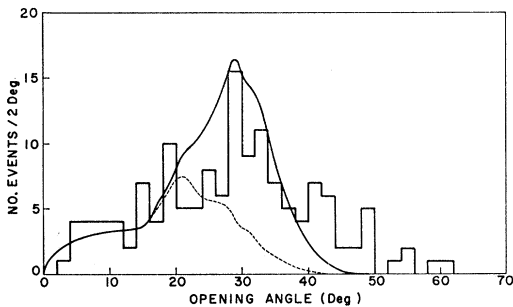


FIG. 5. Comparison of the data with the Monte Carlo distribution when electron-pair decays of the ρ and ω are included. The dashed curve is the background contribution.

⁹ R. I. Hess *et al.*, Bull. Am. Phys. Soc. **10**, 1196 (1965).

¹⁰ $\sigma_{\phi} B_{\phi}$ decreases by a factor of 2 if the ϕ production angular distribution is $T/(T+1)^2$, where T is the square of the 4-momentum transfer, rather than our assumed $1+\cos\alpha$.

The fact that the Monte Carlo calculation for our experimental apparatus gives identical opening-angle distributions for the background events and for the vector-meson decays into muon pairs prevents us from separating muon events from pion events on the basis of the experimental data. Hence we rely entirely on the counting rates to establish an upper limit for the muon branching ratios. For a period during which the corrected beam count was 2.4×10^9 pions there was a total of 3179 muon triggers, and 167 muon triggers with 0.56×10^9 pions incident on the empty target. This yields a net muon trigger count of 2450 ± 80 events (the error is purely statistical). If we use an effective cross section of $0.46 \mu\text{b}$ for the muon background processes as calculated by the Monte Carlo program, 2140 ± 680 events are expected. (The error here includes the uncertainty in the normalization.) Then, the maximum number of events which we can reasonably attribute to the direct muon decays is 1070, corresponding to $0.23 \mu\text{b}$. If we attribute all 1070 events to the decay $\rho \rightarrow \mu\bar{\mu}$, then we obtain an upper limit of $B(\rho \rightarrow \mu\bar{\mu}) < 14 \times 10^{-4}$. Similarly, if all are called ω decays, we have $B(\omega \rightarrow \mu\bar{\mu}) < 90 \times 10^{-4}$; and finally for ϕ decays we find $\sigma_{\phi} \times B(\phi \rightarrow \mu\bar{\mu}) < 8.5 \mu\text{b}$.

The dependence of our electron pair-results upon the value used for the ω - ϕ mixing angle θ may be seen from Eqs. (1') and (2'). The most direct way of determining θ is just this type of experiment, i.e., the independent measurement of the decay rates of the ρ , ω , and ϕ mesons into lepton pairs, but the currently available data do not permit such a determination. Calculations based upon other measurements, e.g., the masses of the mesons, have lead to values of θ which

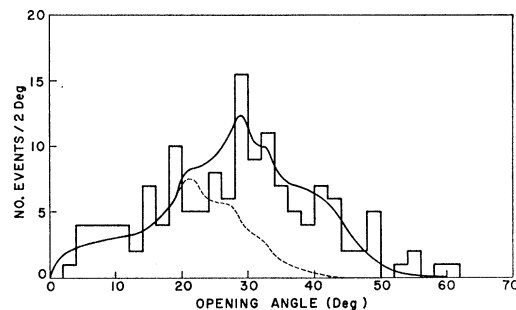


FIG. 6. Data and the Monte Carlo distribution when electron-pair decays of the ϕ , as well as the ρ and ω , are included. The dashed curve is the background contribution for the best fit.

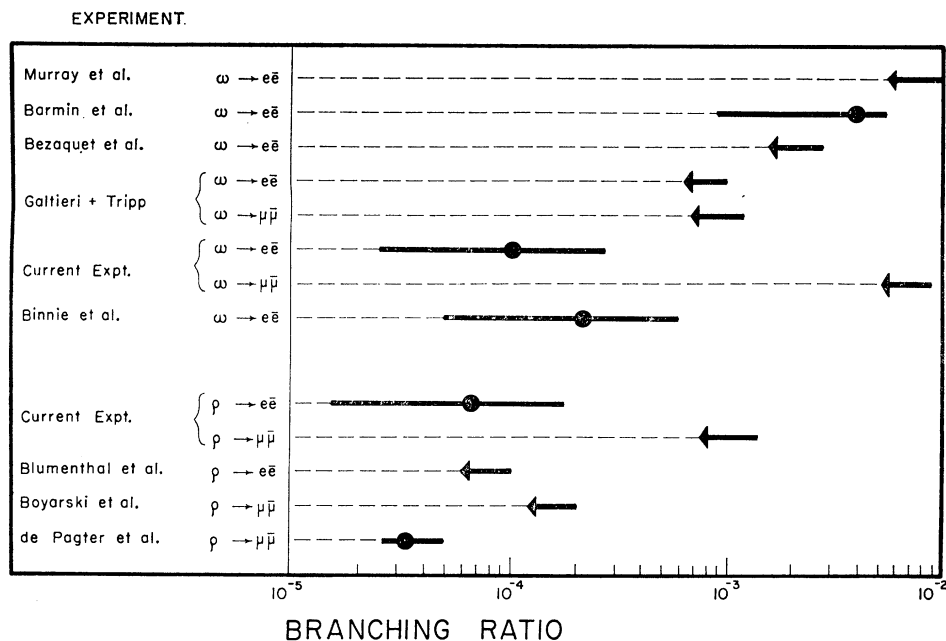


FIG. 7. Comparison of present results with other experiments. (See Refs. 7, 12.)

range from 17° ¹¹ to 38° ^{2,4,5}. In the above calculations we have used the more frequently quoted value of $\theta \approx 38^\circ$. For $\theta = 17^\circ$ our results would be $B_\rho = 0.75 \times 10^{-4}$ and $B_\omega = 0.25 \times 10^{-4}$.

The electron-pair results are an order of magnitude smaller than the limits set by the bubble-chamber experiments. To compare our results for the decays of the ρ and ω mesons with those of other experiments we refer to Fig. 7 where we have tabulated other published results.^{7,12} It is well known² that, if the muon and electron have the same electromagnetic interactions for a time-like momentum transfer of magnitude $\approx M_\nu$, the ratio of the rate for the decay of the meson ν into electron pairs to that for muon pairs should be unity to within terms of order $(M_\mu/M_\nu)^4 \approx 0.1\%$. Thus we may directly compare μ -pair rates with e -pair rates for the same meson and refer to Eq. (2') to compare ρ rates with ω rates. It is seen that the data (with the exception of the result of Barmin *et al.*, which should probably be considered as an upper limit) are consistent

with one another. However, most of the present data have error bars which are too large to allow their use as a determination of the ω - ϕ mixing angle.

ACKNOWLEDGMENTS

We wish to acknowledge many helpful and encouraging discussions with Professor G. Feldman, Professor T. Fulton, Professor A. Pevsner, and Dr. G. Kane. We also want to thank Dr. R. Shutt and members of the staff of the AGS and Johns Hopkins who were instrumental in the execution of this experiment. Finally, we are especially indebted to the Olin Mathieson Chemical Corporation for the aluminum ingots which were used for absorbers in this experiment.

APPENDIX

The shower chambers, together with the B and B* counter arrays, provided electronic identification of electrons and rejection of pion background by virtue

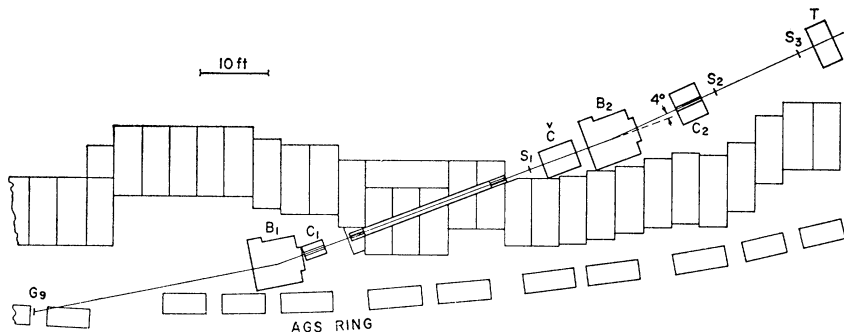


FIG. 8. Experimental arrangement for testing and calibration of the shower chambers.

¹¹ Y. S. Kim, S. Oneda, and J. C. Pati, *Phys. Rev.* **135**, B863 (1964).
¹² R. B. Blumenthal *et al.*, *Phys. Rev. Letters* **14**, 660 (1965); D. M. Binnie *et al.*, *Phys. Letters* **18**, 348 (1965); A. Boyarski, G. Glass, R. C. Chase, and M. Gettner, *Phys. Rev. Letters* **15**, 835 (1965); J. K. dePagter *et al.*, *ibid.* **16**, 35 (1966).

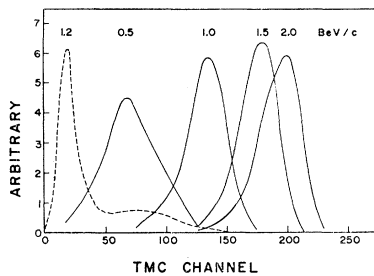


FIG. 9. Pulse-height spectra for sum pulses due to 1.2-BeV/c pions (dashed curve) and electrons (solid curves) of momenta 0.5, 1.0, 1.5, and 2.0 BeV/c (from calibration runs).

of the shower phenomenon. The B and B* counters were constructed of $\frac{1}{2}$ -in.-thick scintillator and covered with $\frac{1}{16}$ -in. aluminum, making a total of 0.07 radiation lengths of material. The A counters were similar, except that the side facing the beam was covered by 1-mil aluminum foil, for 0.05 radiation lengths. The spark chamber T contained $\frac{5}{16}$ in. of aluminum or 0.09 radiation lengths. Each of the counters B and B* was preceded by 1.25 radiation lengths of lead (0.25 in.) in order to initiate shower development. Each of the four chambers consisted of 10 sampling modules composed of 5 sheets of lead (0.028 in.) interleaved with 5 sheets of scintillators ($\frac{1}{8}$ in.). The five scintillators were coupled to a 14-stage photomultiplier tube with a single plastic light pipe. The ten modules were enclosed in an iron box to give a counter having a sensitive area of 20×24-in. and containing 8.5 radiation lengths of material. The signals from the ten photomultiplier dynodes were summed, in a circuit described elsewhere,¹³ to give a sum pulse whose amplitude is a measure of the energy deposited in the chamber. The pulse heights from the individual chamber modules are related to the details of the shower develop-

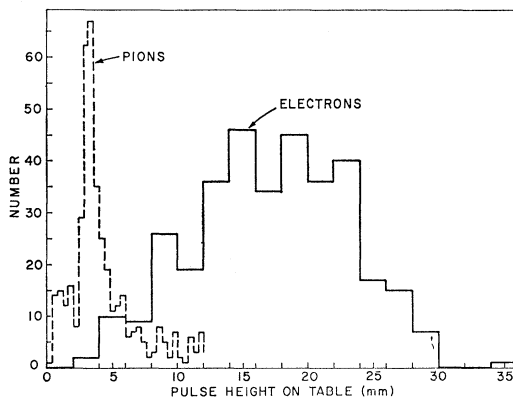


FIG. 10. Pulse-height spectra for sum pulses due to 1.0-BeV/c "electrons" and pions as measured on oscilloscope photographs taken between data runs (see text).

¹³ P. Chagnon, L. Zernow, and L. Madansky, Rev. Sci. Instr. 24, 326 (1953).

ment, and one may use this information to identify electrons.

Tests of this system were made at the Brookhaven AGS in a parasitic beam at G-9-15°. The beam-defining apparatus included two bending magnets and two collimators for momentum selection and a CO₂ gas Čerenkov counter for particle-mass selection. Figure 8 shows the beam layout and counter locations. The bending magnet B2 was set to bend particles of the desired momentum through the 4° angle made by the axes of the collimators C1 and C2, and magnet B1 was set to maximize the flux at this momentum. The total flux at the desired momentum was defined as the triple-coincidence counting rate ($S_1S_2S_3$) and could be normalized relative to a neutron-counting monitor placed inside the AGS shielding wall.

The fourfold coincidence rate ($S_1S_2S_3\check{C}$) was measured as a function of Čerenkov-counter gas pressure and normalized with respect to the total flux ($S_1S_2S_3$) in order to determine the proper pressure settings for particle selection. After all settings had been made, the fourfold coincidence rate was used as the flux of the desired particles at the selected momentum. The counting efficiency of the system T being tested was defined as the ratio of the coincidence rate ($S_1S_2S_3\check{C}T$) to the rate ($S_1S_2S_3\check{C}$).

A TMC multichannel analyzer was used to obtain desired pulse height spectra. The input to the analyzer could be gated by ($S_1S_2S_3\check{C}$) or ($S_1S_2S_3\check{C}T$) in order to obtain the spectrum for the selected particle and momentum. The ten phototube outputs were added, the sum pulse was amplified in a Hewlett-Packard wide-band amplifier, and the resulting signal fed into the gated analyzer. We thus obtained the spectrum of the sum pulse for various particles as a function of momentum. Pulse-height spectra obtained during a calibration run for 1.2-BeV/c pions and electrons of several momenta are shown in Fig. 9.

In practice, pulse-height discrimination on the signals from the anodes of counters B and B* and the first module of the shower chamber provided adequate separation of electrons and pions. The optimum relative discrimination levels were determined to be, respectively, 1.45, 1.6, and 2.3 times the pulse height corresponding to a minimum-ionizing particle. It was with these levels that the counting efficiency curves in Fig. 2 were obtained. These efficiencies were independent of the position and angle of incidence (up to 30°) of the beam. Sufficient measurements were made to enable the results to be reproduced during the data-taking runs. Figure 10 displays pulse-height spectra for 1.0-BeV/c "electrons" and pions as measured on oscilloscope photographs taken for calibration between data-taking runs. For these photographs "electrons" were defined by the electron-identifying pulse-height requirements stated above.